Dynamic Analysis of a Reciprocating Compression Mechanism Considering Hydrodynamic Forces

Tae-Jong Kim*

School of Mechanical Engineering and Research Institute of Mechanical Technology, Pusan National University, Pusan 609-735, Korea

In this paper, a dynamic analysis of the reciprocating compression mechanism of a small refrigeration compressor is performed. In the problem formulation of the mechanism dynamics, the viscous frictional force between the piston and the cylinder wall is considered in order to determine the coupled dynamic behaviors of the piston and the crankshaft. Simultaneous solutions are obtained for the equations of motion of the reciprocating mechanism and the time-dependent Reynolds equations for the lubricating film between the piston and the cylinder wall and for the oil films on the journal bearings. The hydrodynamic forces of the journal bearings are calculated by using a finite bearing model along with the Gümbel boundary condition. A Newton-Raphson procedure is employed in solving the nonlinear equations for the piston and crankshaft. The developed computer program can be used to calculate the complete trajectories of the piston and the crankshaft as functions of the crank angle under compressor-running conditions. The results explored the effects of the radial clearance of the piston, oil viscosity, and mass and mass moment of inertia of the piston and connecting rod on the stability of the compression mechanism.

Key Words : Reciprocating Compressors, Piston Secondary Dynamics, Crankshaft-Journal Bearing System, Hydrodynamic Force, Dynamic Behavior

1. Introduction

Compressor manufacturing is characterized by mass production, and therefore a method for predicting the dynamic behaviors of the compression mechanism is required to enhance compressor performance and reliability, and to save time at the design stage. A reciprocating compressor employed in refrigeration appliances utilizes the slider-crank mechanism, which consists of a piston, a connecting rod, and a crankshaft. Due to the inherent nature of this mechanism, the dynamic behaviors of the compressor unit are assumed to influence each other. Therefore, a coupled dynamic analysis of the compression mechanism is needed. Until now, most studies on the dynamic analysis of a reciprocating mechanism have not been concerned with the interaction between the piston and the crankshaft due to the inclusion of the viscous frictional force of a piston. The reason is that the analysis requires simultaneous solutions of the equations of the motion of the piston, connecting rod, and crankshaft along with the time-dependant Reynolds equations for the lubricating film between the piston and the cylinder wall and for the oil films of the journal bearings.

Refrigeration-reciprocating compressors employ ringless pistons to eliminate the friction between the piston and the cylinder wall because they allow only small amounts of friction loss. Thus, the length of the cylinder bore tends to decrease for diminishing the frictional loss of the piston-cylinder system. Since the ring-less piston

* **E-mail** : tjong@pusan.ac.kr
TEL : +82-51-510-2474; **FAX** : +82-51-514-7640
School of Mechanical Engineering and Research Institute of Mechanical Technology, Pusan National University, Pusan 609-735, Korea. (Manuscript **Received** October 15, 2002; **Revised** April 8, 2003)

is free to move laterally, there is the potential danger of the piston hitting the cylinder wall while moving up and down along its axis. A good design must therefore provide for a smooth and stable reciprocating motion of the piston and ensure that the oil film separating the piston from the cylinder wall is maintained at all times. From a dynamic model of the secondary motion of the piston, the viscous frictional force of the piston in the axial direction can be obtained by a hydrodynamic analysis solving the Reynolds equation for the oil film. From a literature review, this friction force is calculated by simply assuming the Coulomb friction coefficients μ=0.03 (Ishii et al., 1975) and μ=0.35 (Dufour et al., 1995). It is difficult to assume the range of this coefficient without an experimental procedure. Therefore a dynamic analysis of the secondary motion of the piston is required in order to derive a viscous friction force, which can be regarded as theoretically reasonable and accurate. Early studies on piston slap model by Li, et al.(1983) and Zhu, et al.(1992) solved the problem for the reciprocating piston in automotive engines. There is another method (Nakada et al., 1997 ; Cho et al., 2000) for calculating the piston impact forces by utilizing the equivalent mass, damping, and stiffness of the cylinder wall at the contact points. There are a couple of studies (Prata et al., 2000 ; Kim, 2003) on the secondary dynamics of ringless piston regarding reciprocating compressors.

The oscillating motion of the piston in the cylinder bore and the crankshaft whirl in the journal bearings are directly related to the hydrodynamic characteristics of the fluid films of the piston-cylinder clearance and journal clearances. It is certainly necessary to develop and improve hydrodynamic analysis of the fluid films for better understanding compression mechanism dynamics and for reliable prediction of the friction characteristics. Many methods for solving the journal orbit of dynamically loaded journal bearings are available : the short bearing assumption method (Kirk and Gunter, 1975); the mobility method (Booker, 1971) utilizing the stored bearing characteristics ; FEM (Goenka, 1984). The solution of the Reynold's equation can be numerically determined using a finite volume method and the Elrod cavitation algorithm (Brewe, 1986 ; Kim and Han, 1998) can also be applied. However it is difficult to obtain the value of the bulk modulus (compressibility factor) of the lubricant easily and exactly.

In this study, a problem formulation for the nonlinear dynamics of the reciprocating compression mechanism is presented, which considers the viscous frictional force of piston with the contact length of the piston-cylinder system varied. The dynamic load capacity of the journal bearings is calculated by using a finite bearing model and the Gümbel boundary condition. The developed computer program is able to calculate the entire trajectory of the piston and the crankshaft as well as the hydrodynamic forces and moments as functions of the crank angle under compressor-running conditions. The numerical results also showed the effects of the radial clearance of the piston, the lubricant viscosity, and the mass and mass inertia moment of the piston and connecting rod on the dynamic stability of the compression mechanism.

2. Dynamic Formulation

2.1 Piston secondary dynamics

A piston-cylinder system in the reciprocating compressors is shown in Fig. 1(a) and the equations describing the piston secondary dynamics can be written in dimensionless form as

$$\bar{T}_y+\bar{F}_h=\bar{m}_p\ddot{\bar{y}}_0 \tag{1}$$

$$\bar{M}_f+\bar{M}_h=\bar{I}_p\ddot{\bar{\gamma}} \tag{2}$$

$$\bar{m}_p=\frac{\omega C_p^3}{\lambda R_p^4}m_p,\ \bar{y}_0=\frac{y_0}{C_p},\ \bar{\gamma}=\frac{R_p}{C_p}\gamma,\ \bar{I}_p=\frac{\omega}{\lambda R_p^3}\left(\frac{C_p}{R_p}\right)^3 I_p,$$
$$\bar{T}_y=\frac{T_y}{\lambda\omega R_p^2}\left(\frac{C_p}{R_p}\right)^2,\ \bar{F}_h=\frac{F_h}{\lambda\omega R_p^2}\left(\frac{C_p}{R_p}\right)^2,$$
$$\bar{M}_h=\frac{M_h}{\lambda\omega R_p^3}\left(\frac{C_p}{R_p}\right)^2,\ \bar{M}_f=\frac{M_f}{\lambda\omega R^3}\left(\frac{C_p}{R_p}\right)^2$$

where T_y is the excitation force upon the piston (Kim, 2002), m_p is the mass of the piston, R_p is the radius of the piston, C_p is the radial clearance, and λ is the viscosity of the lubricant oil. F_h is the

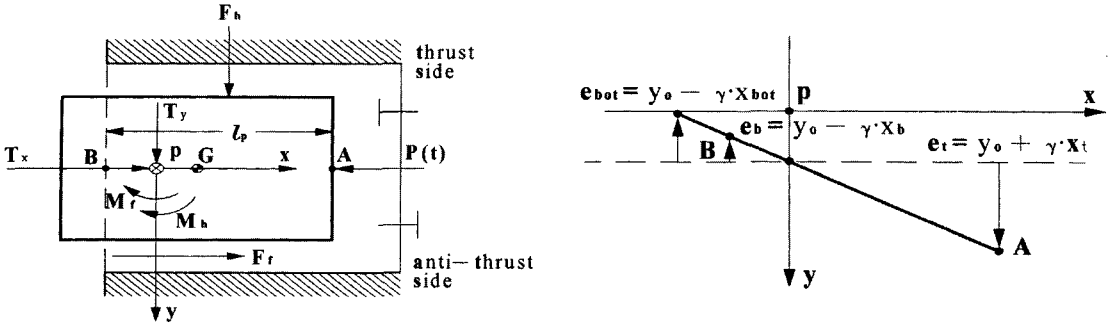

Fig. 1 Free body diagram of the reciprocating piston

hydrodynamic force of the oil film, M_f and M_h are, respectively, the moments about the piston-pin due to F_f and F_h, and y_0 and γ are, respectively, the translatory and rotary displacements of the piston. The boundary position B of the piston is not in-fixed if the sum of the piston length and stroke exceeds the length of the cylinder bore. The nondimensional accelerations $\ddot{\bar{y}}_0$ and $\ddot{\bar{\gamma}}$ can be obtained from the lateral accelerations $\ddot{\varepsilon}_t$ and $\ddot{\varepsilon}_b$ of the two ends, A and B, of the reciprocating piston in Fig. 1(b), as

$$\ddot{\bar{y}}_0=\ddot{\varepsilon}_b-\left(\frac{\ddot{\varepsilon}_b-\ddot{\varepsilon}_t}{\bar{l}_p}\right)\bar{x}_b \tag{3}$$

$$\ddot{\bar{\gamma}}=(\ddot{\varepsilon}_t-\ddot{\varepsilon}_b)/\bar{l}_p$$

$$\bar{l}_p=\frac{l_p}{R_p},\ \bar{x}_b=\frac{x_b}{R_p},\ \varepsilon_b=\frac{e_b}{C_p},\ \varepsilon_t=\frac{e_t}{C_p} \tag{4}$$

where l_p designates the contacting length between the piston and the cylinder wall, x_b is the distance from the origin p of the xyz coordinates to the piston boundary surface B. And, ε_b and ε_t are the dimensionless eccentricities of the bottom and top of the piston, respectively. Therefore, a merging of the above equations (3), (4) with (1), (2) yields the following nonlinear equation system,

$$f_1(\dot{\varepsilon}_b,\ \dot{\varepsilon}_t)=\bar{T}_y+\bar{F}_h-\bar{m}_p\left[\ddot{\varepsilon}_b-(\ddot{\varepsilon}_b-\ddot{\varepsilon}_t)\frac{\bar{x}_b}{\bar{l}_p}\right]=0 \tag{5}$$

$$f_2(\dot{\varepsilon}_b,\ \dot{\varepsilon}_t)=\bar{M}_f+\bar{M}_h-\bar{I}_p(\ddot{\varepsilon}_t-\ddot{\varepsilon}_b)/\bar{l}_p=0 \tag{6}$$

2.2 Crankshaft dynamics

From the analytical model of the crankshaft supported by two journal bearings as shown in Fig. 2(a), the nondimensional equations of motion considering the unbalanced load due to the eccentric mass of the crankshaft, motor rotor and gyro moments of the motor rotor can be derived,

$$\bar{m}_e\ddot{\bar{X}}_0=-\bar{S}_x+\bar{F}_{bx}-\bar{m}_eE_u\cos(\bar{t}+\varphi) \tag{7}$$

$$\bar{m}_e\ddot{\bar{Y}}_0=-\bar{S}_y+\bar{F}_{by}-\bar{m}_eE_u\sin(\bar{t}+\varphi) \tag{8}$$

$$\bar{I}_x\ddot{\bar{\alpha}}=-\bar{I}_z\dot{\bar{\beta}}+\bar{M}_x+\bar{M}_{bx} \tag{9}$$

$$\bar{I}_y\ddot{\bar{\beta}}=\bar{I}_z\dot{\bar{\alpha}}+\bar{M}_y+\bar{M}_{by} \tag{10}$$

$$\bar{m}_e=\frac{\omega C^3}{\lambda R^4}m_e,\ E_u=\frac{r_e}{C},\ \bar{X}_0=\frac{X_0}{C},\ \bar{Y}=\frac{Y_0}{C},\ \bar{t}=\omega t,\ \bar{\alpha}=\frac{\alpha}{C/R},$$

$$\bar{\beta}=\frac{\beta}{C/R},\ \bar{I}=\frac{\omega}{\lambda R^3}\left(\frac{C}{R}\right)^3I,\ \bar{S}_x=\frac{S_x}{\lambda\omega R^2}\left(\frac{C}{R}\right)^2,$$

$$\bar{S}_y=\frac{S_y}{\lambda\omega R^2}\left(\frac{C}{R}\right)^2,\ \bar{M}_x=\frac{M_x}{\lambda\omega R^3}\left(\frac{C}{R}\right)^2,\ \bar{M}_y=\frac{M_y}{\lambda\omega R^3}\left(\frac{C}{R}\right)^2$$

where S_x and S_y are the load forces upon the crankshaft (Kim, 2002), m_e is the eccentric mass of the crankshaft and motor rotor, φ is the phase angle of the eccentric mass, r_e is the eccentric radius of the crankshaft mass, C is the radial clearance of the journal bearings, R is the crankshaft radius on bearings, and where the load moments are calculated by $\begin{Bmatrix}M_x\\M_y\end{Bmatrix}=\mp\begin{Bmatrix}S_x\\S_y\end{Bmatrix}L_f$.

Making use of Fig. 2(b), the nondimensional translation accelerations $\ddot{\bar{X}}_0$, $\ddot{\bar{Y}}_0$ and rotation accelerations $\ddot{\bar{\alpha}}$, $\ddot{\bar{\beta}}$ can be expressed from the lateral accelerations $\ddot{\varepsilon}_{1x}$, $\ddot{\varepsilon}_{2x}$, $\ddot{\varepsilon}_{1y}$, $\ddot{\varepsilon}_{2y}$ of two locations D, E of the crankshaft,

$$\ddot{\bar{X}}_0=\ddot{\varepsilon}_{2x}-\frac{\ddot{\varepsilon}_{2x}-\ddot{\varepsilon}_{1x}}{\bar{L}_b}\cdot\bar{L}_{b2} \tag{11}$$

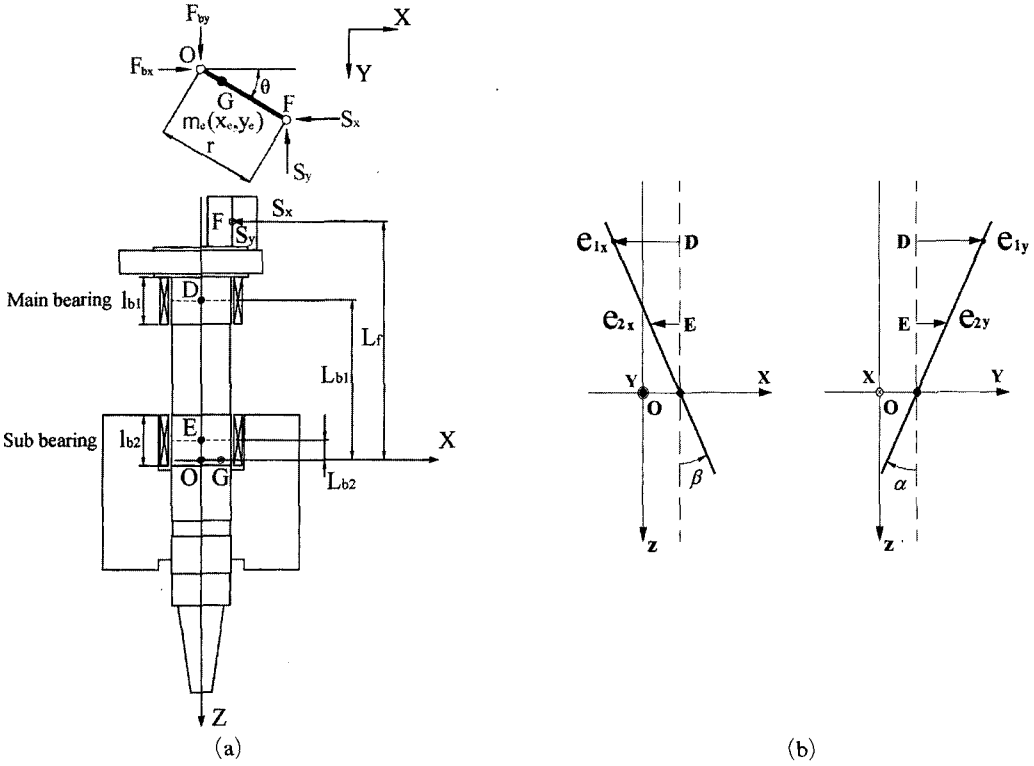

Fig. 2 Analytical model of the crankshaft-journal bearing system

$$\ddot{\bar{Y}}_0=\ddot{\varepsilon}_{2y}+\frac{\ddot{\varepsilon}_{1y}-\ddot{\varepsilon}_{2y}}{\bar{L}_b}\cdot\bar{L}_{b2} \tag{12}$$

$$\ddot{\bar{\alpha}}=\frac{\ddot{\varepsilon}_{1y}-\ddot{\varepsilon}_{2y}}{\bar{L}_b} \tag{13}$$

$$\ddot{\bar{\beta}}=\frac{\ddot{\varepsilon}_{2x}-\ddot{\varepsilon}_{1x}}{\bar{L}_b} \tag{14}$$

$$\bar{L}_b=\frac{L_b}{R},\ \bar{L}_{b2}=\frac{L_{b2}}{R},$$

$$\varepsilon_{1x}=\frac{e_{1x}}{C},\ \varepsilon_{1y}=\frac{e_{1y}}{C},\ \varepsilon_{2x}=\frac{e_{2x}}{C},\ \varepsilon_{2y}=\frac{e_{2y}}{C}$$

where $L_b=L_{b1}-L_{b2}$ is the distance from the main bearing center D to the sub bearing center E, L_{b2} is the distance from the origin O of the XYZ coordinates to the sub bearing center E. And, $(\varepsilon_{1x}, \varepsilon_{1y})$, $(\varepsilon_{2x}, \varepsilon_{2y})$ are the dimensionless eccentricities of the crankshaft at the main bearing center D and the sub-bearing center E, respectively. Merging equations above (11) ~ (14) with (7) ~ (10), the following nonlinear equation system can be deduced for the application of Newton-Raphson method, as

$$g_1(\dot{\varepsilon}_{1x}, \dot{\varepsilon}_{2x}, \dot{\varepsilon}_{1y}, \dot{\varepsilon}_{2y})$$
$$=-\bar{S}_x+\bar{F}_{bx}-\bar{m}_e\bar{E}_u\cos(\bar{t}+\varphi)-\bar{m}_e\left[\ddot{\varepsilon}_{2x}-\left(\frac{\ddot{\varepsilon}_{2x}-\ddot{\varepsilon}_{1x}}{\bar{L}_b}\right)\bar{L}_{b2}\right]=0 \tag{15}$$

$$g_2(\dot{\varepsilon}_{1x}, \dot{\varepsilon}_{2x}, \dot{\varepsilon}_{1y}, \dot{\varepsilon}_{2y})$$
$$=-\bar{S}_y+\bar{F}_{by}-\bar{m}_e\bar{E}_u\sin(\bar{t}+\varphi)-\bar{m}_e\left[\ddot{\varepsilon}_{2y}-\left(\frac{\ddot{\varepsilon}_{1y}-\ddot{\varepsilon}_{2y}}{\bar{L}_b}\right)\bar{L}_{b2}\right]=0 \tag{16}$$

$$g_3(\dot{\varepsilon}_{1x}, \dot{\varepsilon}_{2x}, \dot{\varepsilon}_{1y}, \dot{\varepsilon}_{2y})=-\bar{I}_z\ddot{\bar{\beta}}+\bar{M}_x+\bar{M}_{bx}-\bar{I}_x\left(\frac{\ddot{\varepsilon}_{1y}-\ddot{\varepsilon}_{2y}}{\bar{L}_b}\right)=0 \tag{17}$$

$$g_4(\dot{\varepsilon}_{1x}, \dot{\varepsilon}_{2x}, \dot{\varepsilon}_{1y}, \dot{\varepsilon}_{2y})=\bar{I}_z\ddot{\bar{\alpha}}+\bar{M}_y+\bar{M}_{by}-\bar{I}_y\left(\frac{\ddot{\varepsilon}_{2x}-\ddot{\varepsilon}_{1x}}{\bar{L}_b}\right)=0 \tag{18}$$

3. Hydrodynamic Analysis

3.1 Oil film between piston and cylinder wall

The forces F_f, F_h and moments M_f, M_h acting on the piston skirts are due to the hydrodynamic pressure developed in the oil film between the piston and the cylinder wall, and can be obtained from the Reynolds equation. The Reynolds equation for this incompressible and laminar flow can

be written in nondimensional form as

$$\frac{\partial}{\partial\theta}\left(\bar{h}^3\frac{\partial\bar{p}}{\partial\theta}\right)+\frac{\partial}{\partial\bar{x}}\left(\bar{h}^3\frac{\partial\bar{p}}{\partial\bar{x}}\right)=6\bar{V}_p\frac{\partial\bar{h}}{\partial\bar{x}}+12\frac{\partial\bar{h}}{\partial\bar{t}} \quad (19)$$

$$\bar{h}=1-(\bar{y}_0+\bar{\gamma}\cdot\bar{x}_{i,j})\cos\theta \quad (20)$$

$$\bar{h}=\frac{h}{C_p},\ \bar{x}=\frac{x}{R_p},\ \bar{x}_{i,j}=\frac{x_{i,j}}{R},\ \bar{p}=\frac{p}{\lambda\omega}\left(\frac{C_p}{R_p}\right)^2,\ \bar{V}_p=\frac{V_p}{\omega R_p}$$

where $x_{i,j}$ is the axial distance from the origin p of the xy coordinates to the grid point (i, j) of the bearing surface of the piston, h is the local oil film thickness, and V_p represents piston axial velocity. This equation can be discretized with the conventional finite difference scheme. The hydrodynamic pressure can be calculated by using the SOR (Successive Over Relaxation) method with the over-relaxation parameter ω_c. If the pressure in the oil film is known, then the nondimensional hydrodynamic force $\bar{F}_h$ and moment $\bar{M}_h$ can be determined from, respectively,

$$\bar{F}_h=-\int_0^{2\pi}\int_0^{\bar{l}_p}\bar{p}(\theta,\bar{x})\cos\theta\,d\bar{x}\cdot d\theta \quad (21)$$

$$\bar{M}_h=-\int_0^{2\pi}\int_0^{\bar{l}_p}[\bar{p}(\theta,\bar{x})\cdot\cos\theta]\bar{x}_{i,j}d\bar{x}\cdot d\theta \quad (22)$$

Also, the nondimensional viscous frictional force $\bar{F}_f$ and moment $\bar{M}_f$ can be obtained according to

$$\bar{F}_f=\frac{C_p}{R_p}\int_0^{2\pi}\int_0^{\bar{l}_p}\left(\frac{\bar{h}}{2}\frac{\partial\bar{p}}{\partial\bar{x}}+\frac{\bar{V}_p}{\bar{h}}\right)d\bar{x}\,d\theta \quad (23)$$

$$\bar{M}_f=\frac{C_p}{R_p}\int_0^{2\pi}\int_0^{\bar{l}_p}\left(\frac{\bar{h}}{2}\frac{\partial\bar{p}}{\partial\bar{x}}+\frac{\bar{V}_p}{\bar{h}}\right)\cos\theta\,d\bar{x}\,d\theta \quad (24)$$

3.2 Oil film of journal bearings

The Reynolds equations for the oil films on the journal bearings can be derived in nondimensional form as

$$\frac{\partial}{\partial\theta}\left(\bar{h}_i^3\frac{\partial\bar{p}_i}{\partial\theta}\right)+\frac{\partial}{\partial\bar{z}_i}\left(\bar{h}_i^3\frac{\partial\bar{p}_i}{\partial\bar{z}_i}\right)=6\frac{\partial\bar{h}_i}{\partial\theta}+12\frac{\partial\bar{h}_i}{\partial\bar{t}}\ (i=1,2) \quad (25)$$

$$\bar{h}_i=1-(\varepsilon_{ix}\cos\theta+\varepsilon_{iy}\sin\theta) \quad (26)$$

$$\bar{h}_i=\frac{h_i}{C},\ \bar{z}_i=\frac{z_i}{R},\ \bar{p}_i=\frac{p_i}{\lambda\omega}\left(\frac{C}{R}\right)^2$$

where subscript i designates the bearing number $i=1$ for the main bearing and $i=2$ for the sub bearing, and h_i represents the local oil film thickness of the journal bearings. The hydrodynamic forces and moments may be calculated according to

$$\begin{Bmatrix}\bar{F}_{bxi}\\ \bar{F}_{byi}\end{Bmatrix}=-\int_0^{2\pi}\int_0^{\bar{l}_{bi}}\bar{p}_i(\theta,\bar{z}_i)\begin{Bmatrix}\cos\theta\\ \sin\theta\end{Bmatrix}d\bar{z}_i\,d\theta \quad (27)$$

$$\begin{Bmatrix}\bar{M}_{bxi}\\ \bar{M}_{byi}\end{Bmatrix}=\pm\int_0^{2\pi}\int_0^{\bar{l}_{bi}}\bar{p}_i(\theta,\bar{z}_i)\begin{Bmatrix}\sin\theta\\ \cos\theta\end{Bmatrix}\cdot\bar{Z}_{ij}d\bar{z}_i\,d\theta \quad (28)$$

where $\bar{Z}_{i,j}\left(=\frac{Z_{i,j}}{R}\right)$ is the nondimensional distance from the origin O of the XYZ coordinates to the nodal point of the grid system on the bearing surface. And, $\bar{F}_{bx}$, $\bar{F}_{by}$, $\bar{M}_{bx}$, $\bar{M}_{by}$ are total nondimensional forces and moments on all the bearings, calculated as $\begin{Bmatrix}\bar{F}_{bx}\\ \bar{F}_{by}\end{Bmatrix}=\sum_{i=1}^{2}\begin{Bmatrix}\bar{F}_{bxi}\\ \bar{F}_{byi}\end{Bmatrix}$, $\begin{Bmatrix}\bar{M}_{bx}\\ \bar{M}_{by}\end{Bmatrix}=\sum_{i=1}^{2}\begin{Bmatrix}\bar{M}_{bxi}\\ \bar{M}_{byi}\end{Bmatrix}$.

4. Numerical Procedure and Results

4.1 Numerical procedure

Instead of numerically integrating the second-order governing equations of motion for the piston and the crankshaft, a quasi-Newton method can be applied to the nonlinear systems. The constraint forces T_y, S_y of the compression mechanism are calculated by the Newton-Raphson method and the hydrodynamic forces F_f, F_h and moments M_f, M_h are calculated by the SOR scheme. The hydrodynamic forces and moments of the fluid films between the piston and the cylinder wall and the journal bearings are calculated under transient conditions. If this recursive calculation procedure is converged, then a dynamic analysis of the crankshaft proceeds by calculating the hydrodynamic forces and moments of the journal bearings utilizing the finite bearing model and SOR schemes. The numerical procedure is summarized in Fig. 3.

4.2 Results and discussion

The numerical analysis was carried out for a typical reciprocating compressor used in domestic refrigerators and the baseline values used in the

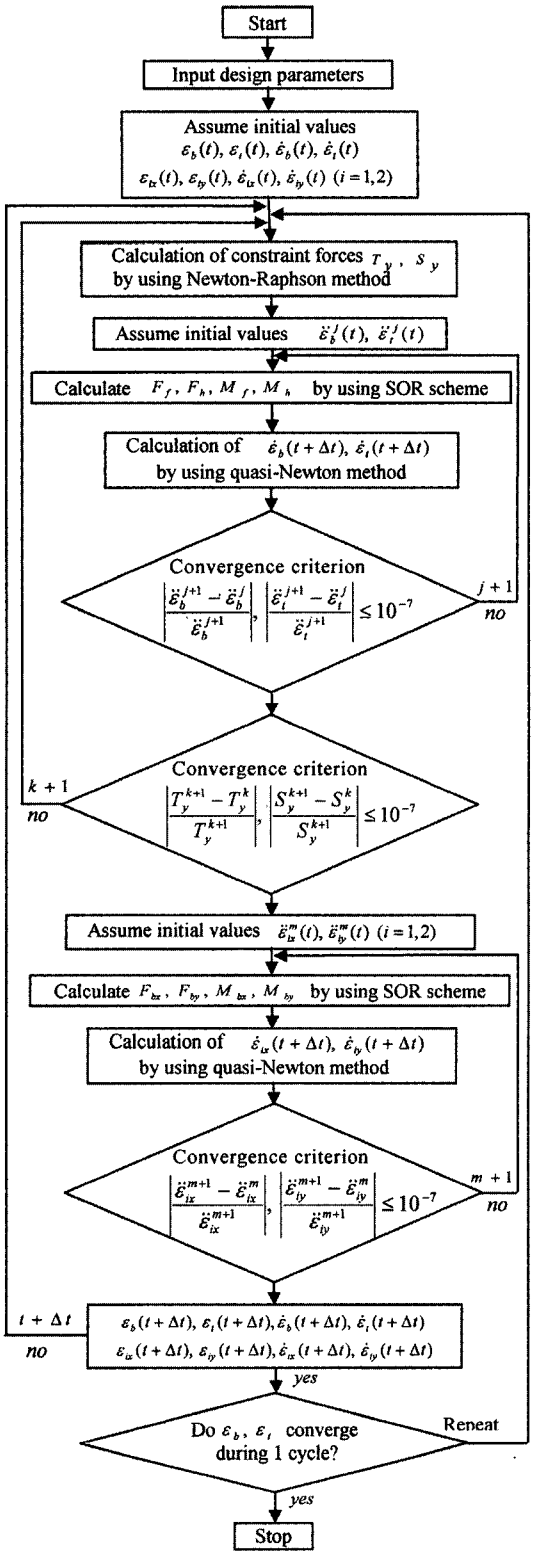

Fig. 3 Flow chart of the calculation procedure

Table 1 Design parameters of the reciprocating compressor and baseline values used in the simulation

Mass of piston (m_p)	0.043 kg
Mass of connecting rod (m_c)	0.24 kg
Mass of crankshaft and motor rotor (m_e)	0.944 kg
Moment of inertia of piston about piston pin (I_p)	3.93×10^{-6} N·m·s^2
Mass moment of inertia of crankshaft and motor rotor about axial gravity center	$I_x=0.82881\times10^{-3}$ N·m·s^2 $I_y=0.8313\times10^{-3}$ N·m·s^2 $I_z=0.3855\times10^{-3}$ N·m·s^2
Radius of piston (R_p)	11.5 mm
Length of piston (L)	22 mm
Length of cylinder wall	28.85 mm
Radial clearance between piston and cylinder wall (C_p)	4 μm
Journal clearance on bearings (C)	11 μm
Lengths of main bearing (l_{b1}) and sub bearing (l_{b2})	13.09 mm, 9.5 mm
Rotating radius of crankshaft	7.5 mm
Lubricant viscosity (λ)	5 mPa·s

simulation are listed in Table 1. The compressor is considered to be operating with a rotation speed of 3570 rpm, a suction pressure of p_s=0.132 MPa and a discharge pressure of p_d=1.352 MPa. Numerical results for the y-direction orbits of the piston center located at the piston top, piston-pin, piston boundary, and piston bottom can be obtained similarly (Kim, 2003; Kim, 2002). The transient loci of the crankshaft center in individual bearings converging within about 2~3 compression cycles under the initial conditions $\varepsilon_{ix}=\varepsilon_{iy}=\dot{\varepsilon}_{ix}=\dot{\varepsilon}_{iy}=0(i=1, 2)$ are shown in Fig. 4. The vertical and horizontal axes represent the eccentricity ratio nondimensionalized by the radial clearance. Most journal bearings are designed to operate with an eccentricity ratio between 0.5 and 0.8, so this crankshaft-journal bearing system can be considered reasonably designed.

Figure 5 shows that the exciting force T_y on the piston is nearly equal to the hydrodynamic reaction force F_h due to the piston inertia's small effect. Also, the viscous frictional moment M_f of the piston is exactly balanced by the hydrody-

namic moment M_h. Similar results can be obtained as shown in Fig. 6. The load forces S_x, S_y upon the crankshaft are dynamically balanced with the hydrodynamic reacting forces F_{bx}, F_{by} if

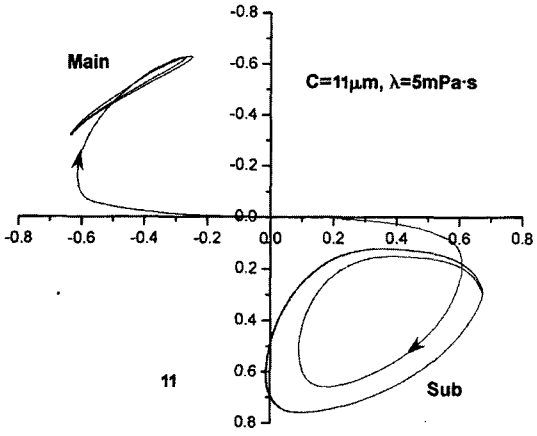

Fig. 4 Transient orbits of the crankshaft at main bearing and sub bearing

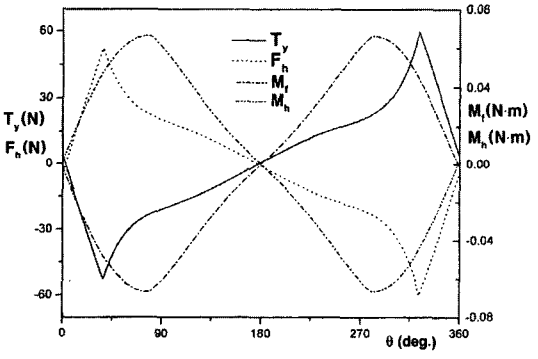

Fig. 5 Applied force T_y, frictional moment M_f, and hydrodynamic force F_h and moment M_h on the piston

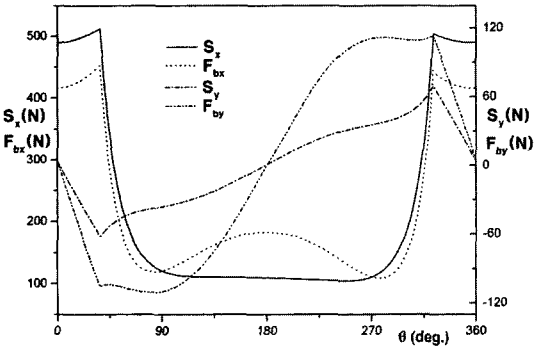

Fig. 6 Applied loads S_x, S_y on the crankshaft and hydrodynamic forces F_{bx}, F_{by} of the journal bearings

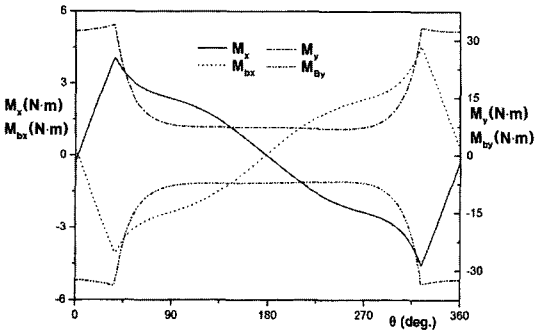

Fig. 7 Load moments M_x, M_y and hydrodynamic moments M_{bx}, M_{by} about the mass center of crankshaft

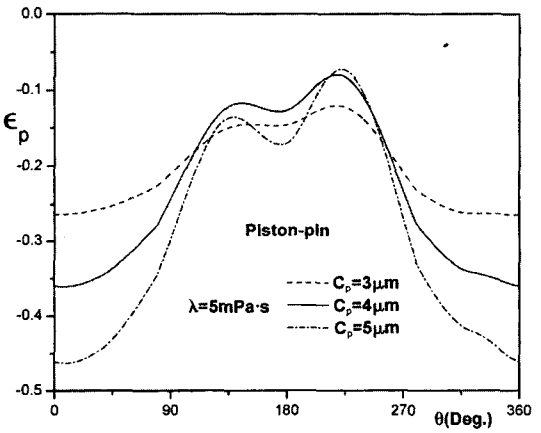

Fig. 8 Comparison of the piston-pin orbits variation in piston clearance

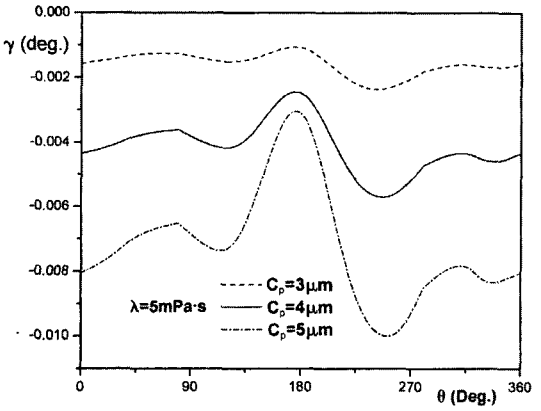

Fig. 9 Comparison of the piston tilting angles variation in piston clearance

the centrifugal forces of the eccentric mass are included. Also, from Fig. 7 the load moments M_x, M_y on the crankshaft about the axial gravity center are well symmetrized to the zero base line of the vertical axis due to the minor effect of the gyro moments of the motor rotor.

The influence of the radial clearance of the piston on the secondary oscillating motion of the piston for the fixed value of viscosity of 5 mPa·s is presented as the orbit at the piston-pin location in Fig. 8 and the tilting angle of the piston in Fig. 9. From these results, reducing the value of the radial clearance results in increasing damping of the oil film, which, in turn, tends to stabilize the secondary motion of the piston. But in the case of the crankshaft, this variation of piston clearance does not affect the journal orbit. Figure 10 shows the comparison of the friction forces generated between the piston and the cylinder wall with a variation in piston clearance. This friction force varies sinusoidally similar to the axial velocity of the piston; however the Coulomb friction force is linearly proportional to the load force of the piston. The effects of the oil viscosity on the radial trajectory of the piston and the rotating whirl of the crankshaft are shown in Fig. 11 and Fig. 12, respectively. As these results show, the dynamic behaviors of the piston are unstabilized with the decreasing value of oil viscosity. And, if the value of oil viscosity rises above $\lambda=10$ mPa·s, then the trajectory of the piston is changed from the convex type to the concave type as shown in Fig. 11.

The influences of the mass and the mass moment of inertia of the piston and connecting rod on the lateral behavior of the piston within the cylinder bore are shown in Fig. 13. Also, the effects of the mass and the mass moment of inertia of the piston and connecting rod on the crankshaft orbits are shown in Fig. 14. From Fig. 13, it can be shown that the secondary trajectory of the piston is enlarged and unstabilized as the inertia value of piston and connecting rod increases. The effect on the crankshaft, as shown in Fig. 14, is that the dynamic orbits are stabilized, increasing the inertia effects contrary to the former result of the piston.

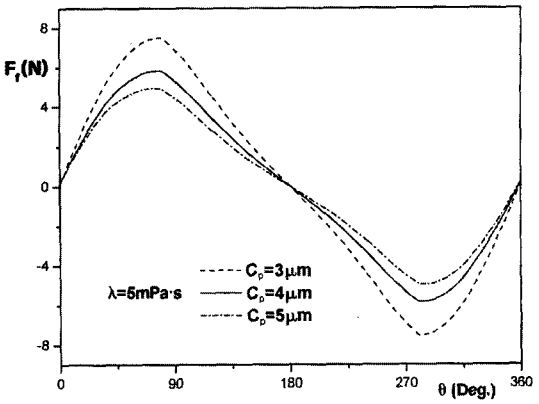

Fig. 10 Comparison of friction forces between piston and cylinder wall variation in piston clearance

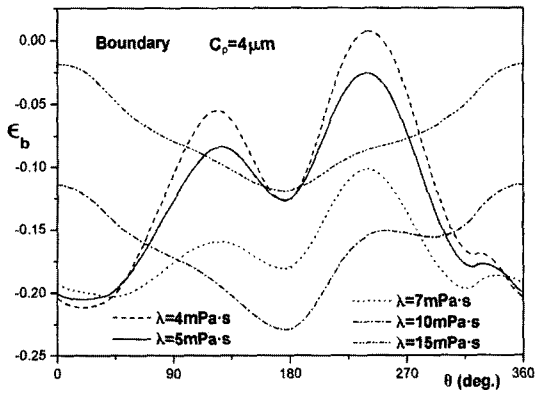

Fig. 11 Comparison of piston-boundary orbits variation in lubricant viscosity

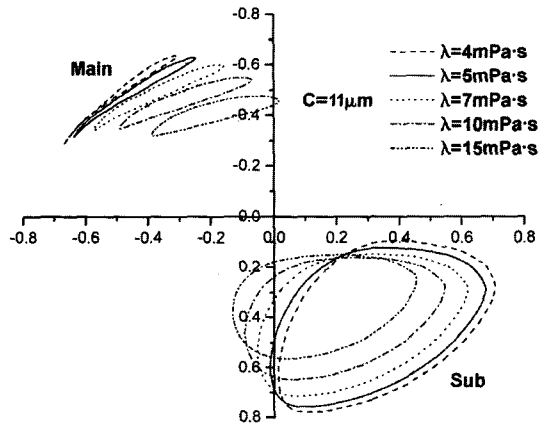

Fig. 12 Comparison of the crankshaft orbits on main bearing and sub bearing variation in in the lubricant viscosity

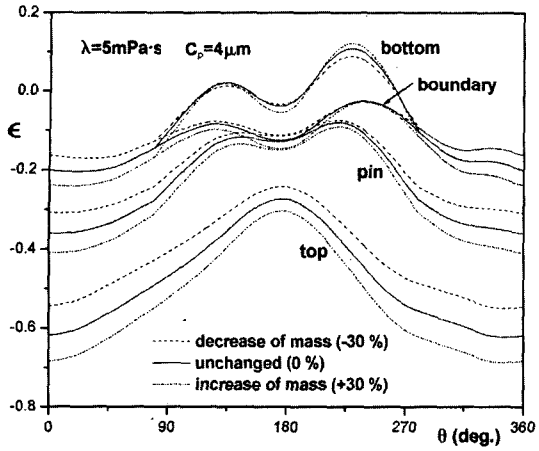

Fig. 13 Comparison of the trajectories of the piston bottom, boundary, pin, and top locations variation in the mass of piston and connecting rod

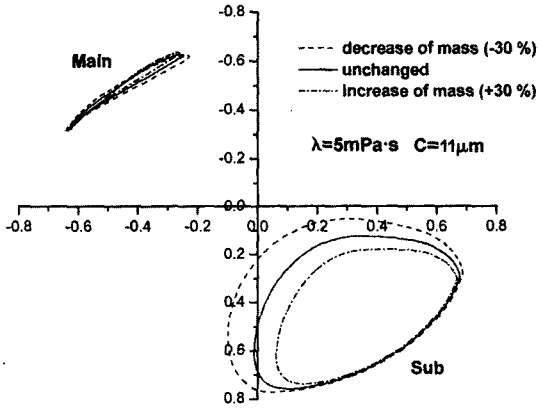

Fig. 14 Comparison of the crankshaft orbits on main bearing and sub bearing variation in the mass of piston and connecting rod

5. Conclusions

A numerical analysis was performed for the dynamics of the reciprocating compression mechanism considering the viscous frictional force of the piston. The analysis incorporated the dynamic equations for the piston and crankshaft as well as the hydrodynamic equations applied to the oil film between the piston and cylinder wall and journal bearings. A computer program based on this mathematical model could be used to analyze the coupled dynamic characteristics of the compression mechanism by calculating the trajectories of the piston and the crankshaft. The effects of the radial clearance of the piston, oil viscosity, mass and mass moment of inertia of the piston and connecting rod on the compression mechanism dynamics were investigated. Among the results, it was shown that a stable piston trajectory can be obtained if the piston clearance is reduced or the value of oil viscosity is increased or the mass and mass moment of inertia of the piston and connecting rod are decreased. It was also found that the crankshaft stability can be improved by increasing the value of the oil viscosity or increasing the mass and mass moment of inertia of the piston and connecting rod. The program presented can be used as a helpful tool in assessing the influence of design parameters on the stability of a reciprocating compressor mechanism.

Acknowledgment

This work was supported by grant No. R01-2001-00383 from the Korea Science & Engineering Foundation.

References

Booker, J. F., 1971, "Dynamically-Loaded Journal Bearings: Numerical Application of the Mobility Method," *ASME Journal of Lubrication Technology*, January, pp. 168~176.

Brewe, D. E., 1986, "Theoretical Modeling of the Vapor Cavitation in Dynamically Loaded Journal Bearings," *ASME Journal of Tribology*, Vol. 108, pp. 628~638.

Cho, S. H., Ahn, S. T. and Kim, Y. H., 2000, "A Model of Collision Point to Estimate Impact Force Related to Piston Slap," *Journal of KSNVE*, Vol. 10, No. 3, pp. 474~479. (In-Korean)

Dufour, R., Hagopian, J. Der and Lalanne, M., 1995, "Transient and Steady State Dynamic Behavior of Single Cylinder Compressors: Prediction and Experiments," *Journal of Sound and Vibration*, Vol. 181, No. 1, pp. 23~41.

Goenka, P. K., 1984, "Dynamically Loaded Journal Bearings: Finite Element Method Analysis," *ASME Journal of Tribology*, Vol. 106,

pp. 429~439.

Ishii, N., Imaichi, K., Kagoroku, N. and Imasu, K., 1975, "Vibration of a Small Reciprocating Compressor," *ASME Paper* 75-DET-44.

Kim, T. J. and Han, D. C., 1998, "Dynamic Behavior Analysis of Scroll Compressor Crankshaft Considering a Cavitation Phenomenon in Dynamically Loaded Journal Bearings," *Transaction of KSME*, A, Vol. 22, No. 8, pp. 1375~1389.

Kim, T. J., 2003 "Numerical Analysis of the Piston Secondary Dynamics in Reciprocating Compressor," *KSME International Journal*, Vol. 17, No. 3, pp. 350~356.

Kim, T. J., 2002, "Dynamic Analysis of the Small Reciprocating Compressors Considering Viscous Frictional Force of a Piston," Journal of KSNVE, Vol. 12, No. 11, pp. 904~913. (In-Korean)

Kirk, R. G. and Gunter E. J., 1975, "Short Bearing Analysis Applied to Rotor Dynamics, Part 1 : Theory," *Journal of Lubrication Technology*, April, pp. 319~329.

Li, D. F., Rohde, S. M. and Ezzat, H. A., 1983, "An Automotive Piston Lubrication Model," *ASLE Transactions*, Vol. 26, No. 2, pp. 151~160.

Nakada, T., Yamamoto, A. and Abe, T., 1997, "A Numerical Approach for Piston Secondary Motion Analysis and its Application to the Piston Related Noise," *SAE paper* No. 972043.

Prata, A. T., Fernando Julio R. S. and Fagotti, F., 2000, "Dynamic Analysis of Piston Secondary Motion for Small Reciprocating Compressors," *Trans. ASME, Journal of Tribology*, Vol. 122, pp. 752~760.

Zhu, D., Cheng, H. S., Arai, T. and Hamai, K., 1992, "A Numerical Analysis for Piston Skirts in Mixed Lubrication Part 1 : Basic Modeling," *Journal of Tribology*, Vol. 114, pp. 553~562.